

Radar-Camera Sensor Fusion Based Object Detection for Smart Vehicles

Eugin Hyun

ART Lab.,
DGIST,
Daegu, Korea
e-mail: braham@dgist.ac.kr

Young-Seok Jin

ART Lab.,
DGIST,
Daegu, Korea
e-mail: ysjin@dgist.ac.kr

Hyeong-Cheol Jeon

ART Lab.,
DGIST,
Daegu, Korea
e-mail: hamtooree@dgist.ac.kr

Young-Nam Shin

DAS Engineering Team,
SL Corporation,
Gyeongsanbuk-do, Korea
e-mail: ynshin@slworld.com

Abstract—We propose a post-data processing scheme for radar sensors in a fusion system consisting of a camera and radar sensors. The proposed scheme is divided into the recursive least square filter, the ghost target and clutter cancellation, and region of interest (ROI) selection. Especially for the recursive least square filter, we determine whether detections are valid tracks or are new tracks to initialize or update the filter parameters. Next, we apply the valid detections to the filter to reduce detection errors. Next, we cancel ghost targets as comparing the current tracks and the last tracks, and suppress clutter using the detected radial velocity. Finally, we select the ROI and determine the transfer coordinates to provide these values to the camera sensor. To verify the proposed method, we use Delphi commercial radar and carry out the measurements in a chamber and on the real road.

Keywords- Post processing; Sensor fusion; ADAS.

I. INTRODUCTION

At present, the Advanced Driver Assistance System (ADAS) is one of the main issues for smart vehicle safety in road traffic. To support effective ADASs, the target detection sensors used are very important. Among currently available sensors, camera and radar sensors are commonly used in ADASs [1][2].

Because radar detects objects by emitting radio signals and analyzing the echo in the reflected signal, this system can operate robustly in different weather conditions [1][2]. Cameras are also widely used because they can provide rich data, similar to that by the human eye [1][2]. However, radar measurements are limited in terms of the angle resolution and this data is rather noisy due to false alarms. Cameras are also sensitive to light and weather conditions, and they have low detection accuracy levels, such as for the velocity and range detections.

Owing to these limitations, sensor fusion technology is considered as an efficient means of increasing target detection performance levels [1]-[3]. Because previous works have provided sensor fusion outcomes in the end stage [4][5], the computational complexity of camera classification remains high. Thus, in order to improve the detection performance and reduce the computational intensity, early-stage-based sensor fusion was proposed in previous works [6]-[8].

In the previous works [6][7], radar is used to detect targets in the region of interest (ROI) of captured image and searches for vehicle features within the ROI. However, the detection

accuracy is unsatisfactory because the camera sensor detects the range of ROI as the pre-processing. In order to overcome the limitation, in another work [8], a more robust and efficient vision-based vehicle detection method was presented. In that case, the radar sensor provides ROIs for the camera sensor. Compared to the [6][7], because the radar sensor detects the range of target, the method can improve the detection accuracy and reduces the false alarm rate.

For the fusion method, the radar system provides precise ROI information to the camera sensor. Specifically, because the coordinates between the radar and the camera have differences, coordinate matching is also required. Finally, because the both sensors' fields of views (FOVs) are also different, the overlap area should be considered.

Thus, in this paper, we propose a radar post-processing scheme, which takes these issues into account for fusion of the camera and radar sensor. Section II briefly presents the proposed radar post-data processing scheme. Section III describes measurement results under the real field. Section IV presents the conclusion.

II. POST-DATA PROCESSING SCHEME

Figure 1 presents the expected fusion results of systems incorporating both camera and radar sensors.

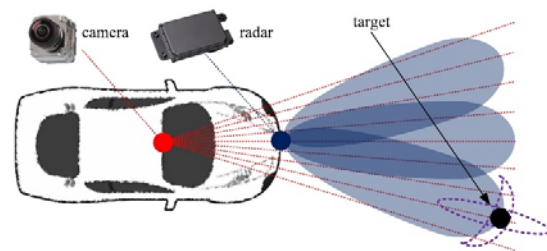


Figure 1. Expected fusion results of camera and radar sensors.

The angle detection of the radar sensor has a low resolution while range detection error of the camera sensor is very high. Here, the overlap between the two sensors is the final detected target position. In order to overcome the limitations of each sensor, we propose the sensor fusion based processing concept shown in Figure 2.

From the radar sensor, the detection information is received through a controller area network (CAN) with radar start command. After packet receiving and decoding, the track

data and the corresponding flag (or status) data are saved in the registers. Subsequently, through the proposed post data processing and projective transformation steps, the ROI information is transferred to the image processing path. In the camera sensor, based on these ROIs, feature extraction and target classification are carried out.

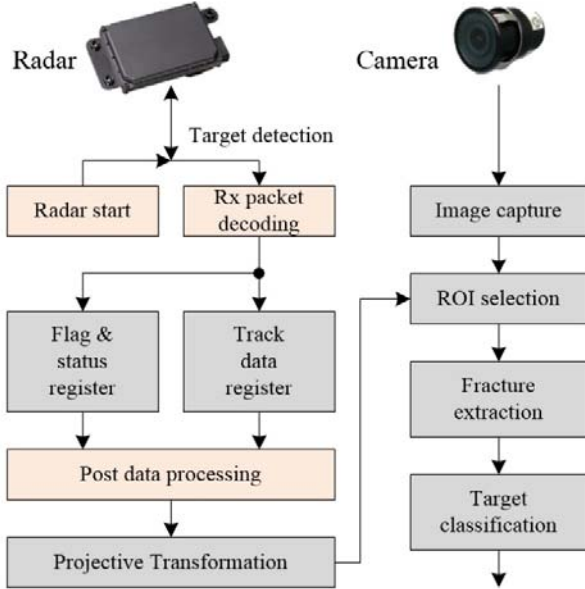


Figure 2. Proposed camera and radar sensor fusion processing concept.

The proposed post data processing scheme for radar is illustrated in Figure 3. First, we determine where detection is valid or not valid using the flag and status values.

In the second step, we initialize the parameters for error minimizing filter if the current track is new. On the other hand, for existing tracks, the corresponding parameters are calculated using the values updated in previous state. In this paper, we employed the recursive least square second order filter [9] to improve the angle detection error. On the other hand, the range and velocity values of the first step are passed without any modifications because the detection errors are very low.

The filter processing is expressed by (1) and (2), where $K1 = 2(2k - 1)/(k^2 + k)$, $K2 = 6/(k^2 + k)$, and $Res = x[k] - \hat{x}[k - 1] - \hat{x}_d[k - 1]$. In this equation, $\hat{x}[k]$ is the k^{th} the estimated angle and $x[k]$ is the k^{th} measurement. For a new track (k is 1), we define $\hat{x}[0] = x[1]$ and $\hat{x}_d[0] = 0$.

$$\hat{x}[k] = \hat{x}[k - 1] + \hat{x}_d[k - 1] + K1 \cdot Res \quad (1)$$

$$\hat{x}_d[k] = \hat{x}_d[k - 1] + K2 \cdot Res \quad (2)$$

Next, the sudden tracks are cancelled. That is, as comparing the current track status and the previous information, we can determine the received detection is ghost or not.

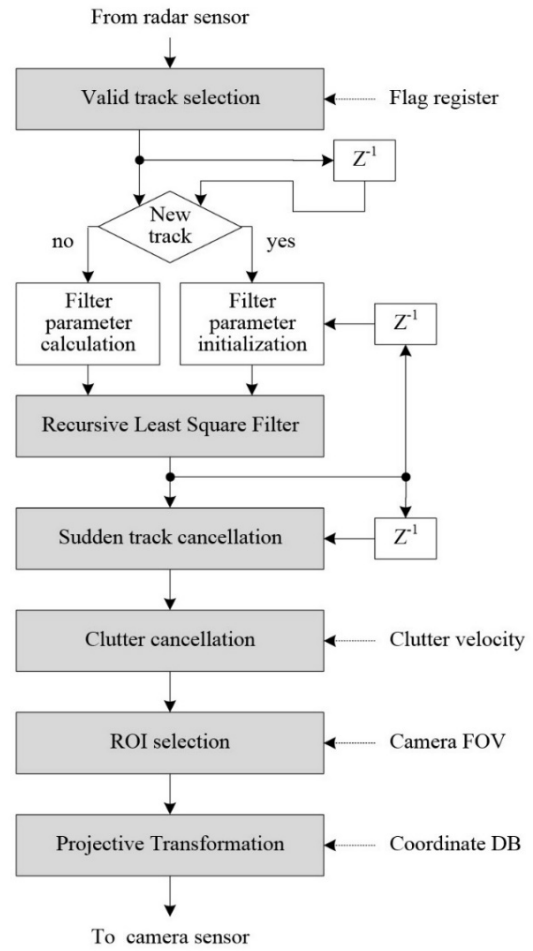


Figure 3. Post-data processing scheme for radar.

In the next step, we distinguish whether the current track is a target or a clutter. If the velocity of the current track, $v[k]$, meets (3), the current track is target, otherwise it can be regard as clutter. Here, v_{min} is maximum velocity of clutter and v_{ego} is ego velocity of subject vehicle. In addition, v_{min} is statistically estimated through the experiment through trade-off between the detection probability and false alarm rate.

$$v[k] < -v_{ego} - v_{min} \text{ or } v[k] > -v_{ego} + v_{min} \quad (3)$$

Then we select the ROI information (range, radial velocity, and angle) in the overlap area of the radar and the camera. Finally, the projective transformation is carried out. In that case, the error bound is also fed to camera sensor considering the range detection error of the camera sensor and angle detection error of the radar sensor. The camera sensor will process images within window size, which reduces the complexity of image processing.

The steps described above are repeated until the scanning of final tracks is completed. The number of tracks is dependent on the type of commercial radar and the corresponding parameter setting.

III. MEASUREMENT RESULTS

In this paper, we employ the *Delphi* 77GHz ESR (Electronically Scanning Radar) system. In this radar system [10], because the maximum number of tracks is 64, the post-data processing described in Section II are repeated until the scanning of 64 tracks is completed.

TABLE I. DELPHI ESR SPECIFICATIONS

| Category | Values |
|--------------------|---------------------------------------|
| Size | 173.7 × 90.2 × 49.2 mm (L × W × H) |
| Weight | 575 g |
| Scanning frequency | 76.5 GHz |
| Field of View | +/- 45° |
| Range | ~ 60m |
| Target | 64 |
| Update rate | <= 50 ms |

In order to verify the post-data processing method for radar, we configured a moving target measurement scenario in a chamber room, as shown in Figure 4. First, we install the *Delphi* ESR on the positioner and a single target is placed on the rail approximately 3.5 m away from the radar. The target then moved from 3.5m to 5.9 m in a round trip.

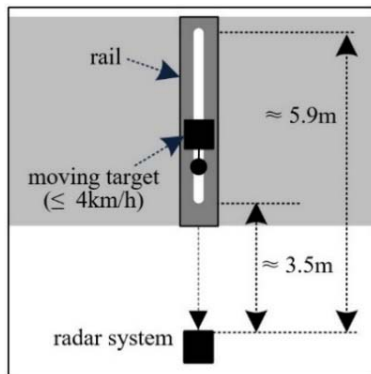


Figure 4. Moving target measurement scenario in chamber room.



Figure 5. Radar measurement set-up.

We also utilized the measurement set-up shown in Figure 5. Here, a PC is connected to the ESR device through CAN to a USB converter. We coded the device driver software to start the radar sensor and data parsing program so as to log the received data using the Matlab simulator. In addition, we also completed the aforementioned post-data processing algorithm.

Figure 6 shows the detection result for several frame times: range (top), radial velocity (middle), and angle (bottom). As shown in the results, the angle detections contain numerous errors. Even when the moving target is placed on the middle line of the radar, the detection results were found to vary. Thus, we filtered the detection outcomes through a recursive least square filter. The corresponding outputs are indicated by the red line in Figure 6.

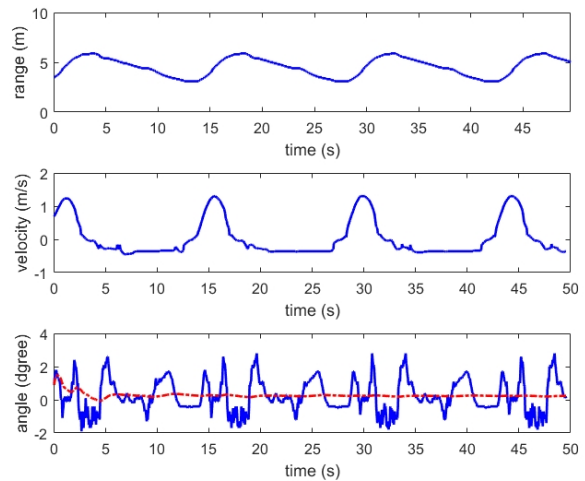
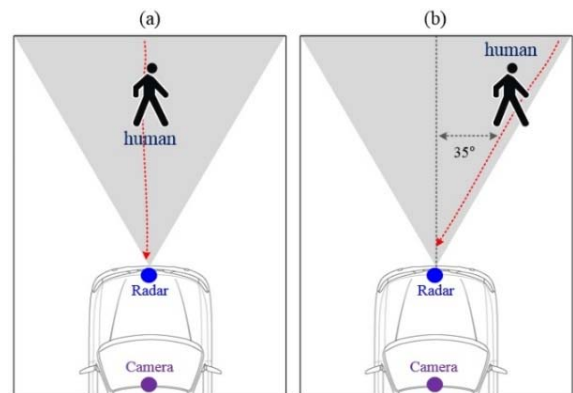


Figure 6. Results of post data processing for radar.

Next, in order to verify the algorithm on the real road, we install the radar and camera on the middle of the vehicle front bumper. The electrical power of vehicle was supplied to the both sensors. Signal lines were built in the vehicle to acquire radar signals and capture camera images together with a PC.

In addition, we considered four scenarios as shown in Figure 7. First, a single human is moving along the middle line of the radar sensor at approximately 6 m (a). In the second scenario (b), a human is walking along the right edge of radar FOV. In next scenario (c), the human is walking 3m away from the middle line in the longitudinal direction. Final case (d) shows the pedestrian who moves laterally at about 3 m away from the radar.



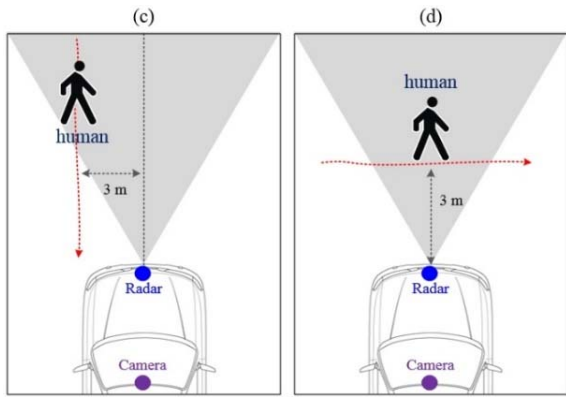


Figure 7. Results of post data processing for radar.

Figures 8-13 present the measurements and post-processing results for each scenario. We monitor moving human for about 7 seconds. In all figures, the blue points are the detected tracks in each frame.

First, Figures 8 and 9 show the results when the human is walking and running for the first scenario, respectively. Here, Figures (a) ~ (c) present the valid tracks received from radar sensor and Figures (d) ~ (f) show the post-data processing results. In Figures (a) and (d), the x-axis is the frame index and the y-axis indicates the range (meter). In Figure (b) and (e), the x-axis indicates the frame index and the y-axis is the angle (degree). Figures 8 (c) and (f) express the corresponding x- and y-positions (meter) of tracks over the whole frames. The results are calculated using range and angle values of each

track. Here, the black line indicates FOV of radar. Figures 9 (c) and (f) show the radial velocity (m/s) over each frame.

In the results of Figure 8, we can see that angle errors are compensated through the recursive least square filter. Moreover, in Figure 9, we can find that the ghost targets and clutter are canceled and the multiple scattering points oriented from one target are grouped together.

Next, in Figures 10, 11, and 12, we present the processing results for the scenarios 2, 3, and 4. In the results, we describe the x-y positions (meter) of target as calculating with the detected range and angle for all frames. We also mark black line to be able to see the detectable angle of radar. From all results, it was proved that the angle errors are minimized, the ghost and clutter were canceled, and the grouping was completed.



Figure 13. Example of ROI selection and window generation for the camera sensor

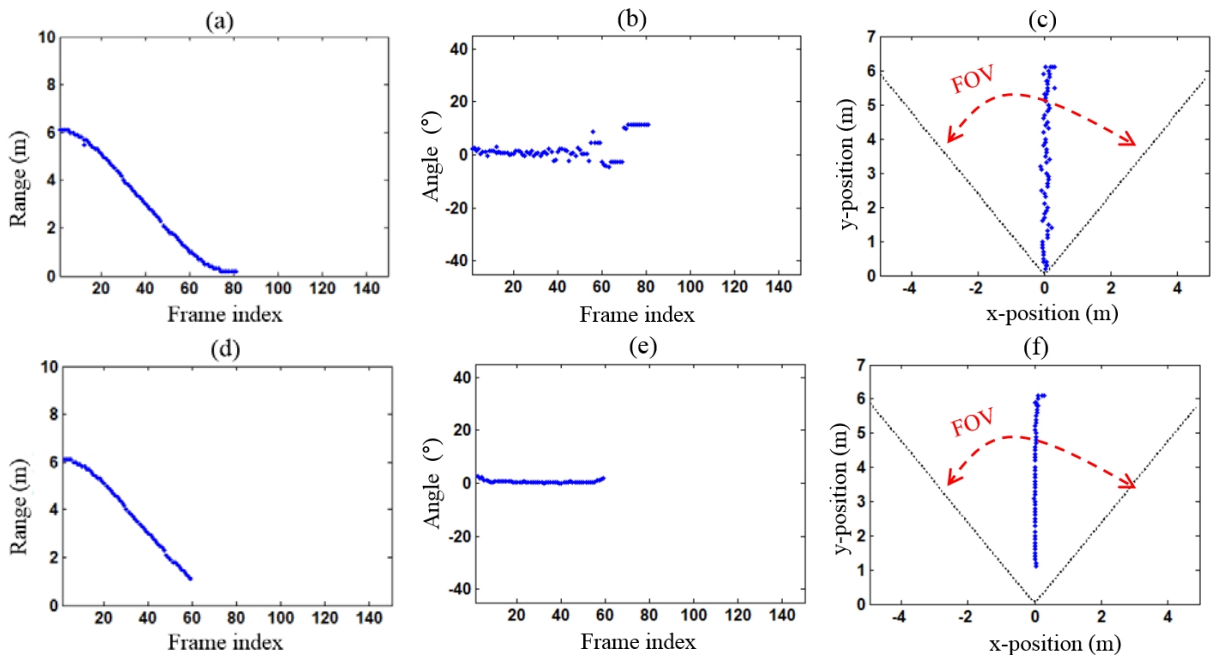


Figure 8. Detected target tracks (range, angle, and the corresponding xy-position) for the first scenario: (a)~(c) tracks before post-processing and (d)~(e) tracks after post-processing.

Last, Figure 13 shows an example of the ROI selection process (red circle) on the captured image for the first scenario. Here, the camera with wide angle was developed by the SL Corporation. In the image processing, the window can be

generated based on selected ROI including the range and angle such the example of Figure 13.

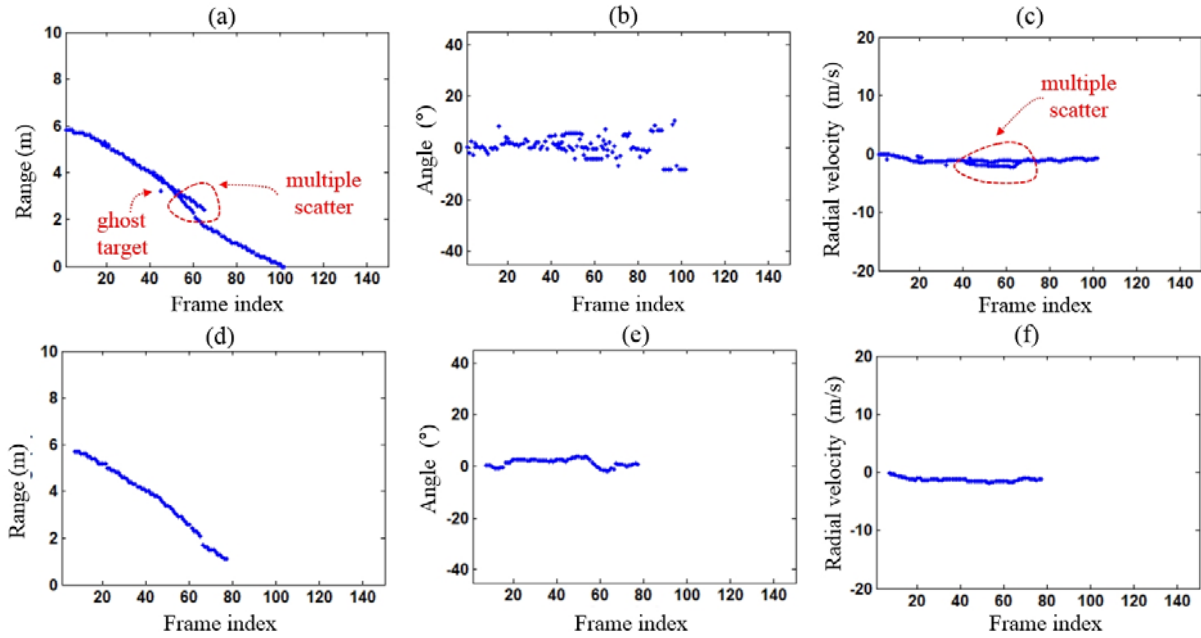


Figure 9. Detected target tracks (range, angle, and radial velocity) for the second scenario: (a)–(c) tracks before post-processing and (d)–(e) tracks after post-processing.

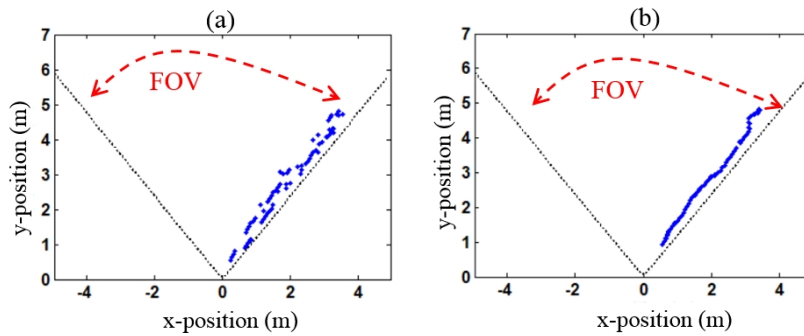


Figure 10. Detected target tracks (xy-position) over the whole frames for the third scenario.

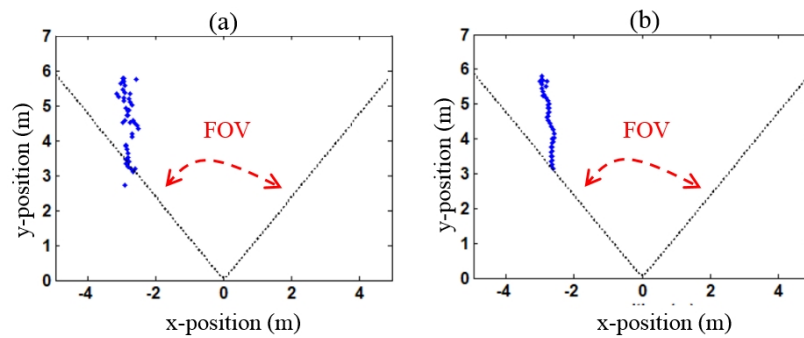


Figure 11. Detected target tracks (xy-position) over the whole frames for the fourth scenario.

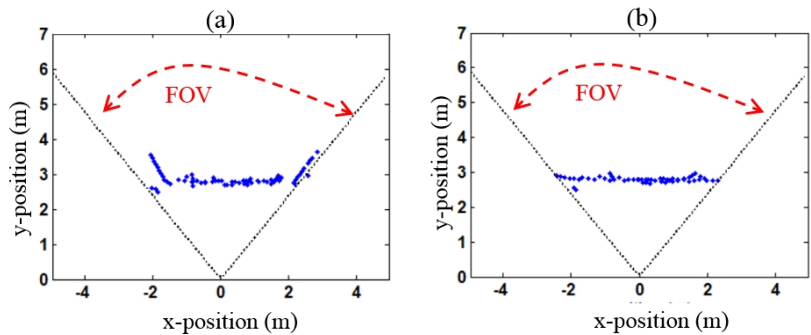


Figure 12. Detected target tracks (xy-position) over the whole frames for the fifth scenario.

IV. CONCLUSION

In this paper, we proposed post radar data processing for a camera and radar sensor fusion system. To do this, we utilized a Delphi 77GHz automotive commercial radar system.

First, using the flag values received from the radar, we determined instances of valid detection and new tracks. Next, we employed a recursive least square filter to reduce the detected angle error. Next we cancelled the ghost target and clutter using the received track information. Finally, based on the selected ROI information, the projective transformation is carried out for the camera sensor. The performance capabilities of the proposed scheme were assessed in a chamber and in the outdoor environment.

In the future, we will verify the proposed processing scheme in various scenarios on the real road. Thus, we will provide the meaningful results. Moreover, together with the camera sensor, we will develop methods of sensor fusion processing. Thus, we will compare the results of sensor fusion and them obtained by camera database alone.

ACKNOWLEDGMENT

This research was supported by the Technology Transfer and Commercialization Program through INNOPOLIS Foundation (2017-DG-0001) and the DGIST R&D Program (18-FA-07) funded by the Ministry of Science and ICT, Korea.

REFERENCES

- [1] A. Gavriilidis, D. Müller, S. Müller-Schneiders, J. Velten, and A. Kummert, "Sensor System Blockage Detection for Night

Time Headlight Control Based on Camera and Radar Sensor Information," IEEE ITSC 2015, Anchorage, USA, Sep. 2012.

- [2] E. Hyun and Y. S. Jin, "Multi-level Fusion Scheme for Target Classification using Camera and Radar Sensors," IPCV'17, Lasvegas, USA, July 2017, pp. 111-114.
- [3] J. Laneurit, C. Blanc, R. Chapuis, and L. Trassoudaine, "Multisensorial data fusion for global vehicle and obstacles absolute positioning," IEEE Intelligent Vehicles Symposium, Columbus, USA, Jun. 2003, pp. 138-143.
- [4] R. O. Chavez-Garcia, J. Burlet, T. D. Vu, and O. Aycard, "Frontal object perception using radar and mono-vision", IEEE Intelligent Vehicles Symposium 2012, Alcalá de Henares, Spain, June 2012
- [5] U. Kadow, G. Schneider, and A. Vukotich, "Radar-vision based vehicle recognition with evolutionary optimized and boosted features," IEEE Intelligent Vehicles Symposium, Istanbul, Turkey, June 2007, pp. 749-754.
- [6] A. Sole, O. Mano, G. Stain, H. Kumon, Y. Tamatsu, and A. Shashua, "Solid or not solid: Vision for radar target validation," IEEE Intelligent Vehicles Symposium, Parma, Italy, Jun. 2004, pp. 819-824.
- [7] G. Alessandretti, A. Broggi, and P. Cerri, "Vehicle and Guard Rail Detection using Radar and Vision Data Fusion," IEEE Transactions on Intelligent Transportation Systems, Vol. 8, Iss. 1, pp. 95-105, Mar. 2007.
- [8] X. Wang, L. Xu, H. Sun, J. Xin, and N. Zheng, "On-Road Vehicle Detection and Tracking Using MMW Radar and Mono-vision Fusion," IEEE Transaction on Intelligent Transportation Systems, Vol. 17, No. 7, pp. 2075-2084, July 2016.
- [9] J. Lee and V. J. Mathews, "A fast recursive least squares adaptive second order Volterra filter and its performance analysis," IEEE Transactions on Signal Processing, Vol. 41, Issue 3, pp. 1087-1102, Mar. 1993.
- [10] Autonomoustuff, "Delphi ESR Startup Guide version 2.1", Oct. 2015.